A 200 Kyr Pleistocene lacustrine record from the Valles Caldera insight: from environmental magnetism and paleomagnetism

Linda Donohoo-Hurley, John W. Geissman, Peter J. Fawcett, Tim Wawrzniec, and Fraser Goff

2007, pp. 424-432. https://doi.org/10.56577/FFC-58.424

in:

Geology of the Jemez Region II, Kues, Barry S., Kelley, Shari A., Lueth, Virgil W.; [eds.], New Mexico Geological Society 58 th Annual Fall Field Conference Guidebook, 499 p. https://doi.org/10.56577/FFC-58

This page is intentionally left blank to maintain order of facing pages.

New Mexico Geological Society Guidebook, 58th Field Conference, Geology of the Jemez Mountains Region II, 2007, p. 424-432.

A 200 KYR PLEISTOCENE LACUSTRINE RECORD FROM THE VALLES CALDERA INSIGHT: FROM ENVIRONMENTAL MAGNETISM AND PALEOMAGNETISM

LINDA DONOHOO-HURLEY, JOHN W. GEISSMAN, PETER FAWCETT, TIM WAWRZYNIEC, AND FRASER GOFF
Department of Earth and Planetary Sciences, MSCO3-2040, 1 University of New Mexico, Albuquerque, New Mexico, 87313; ldonohoo@unm.edu

Abstract — An ~80 m section of lacustrine sediment cored from the Valles Caldera (VC-3) was deposited over three glacial and two interglacial periods in the mid-Pleistocene. An Ar/Ar age determination of 552 $\pm$ 3 ka for an ash layer at 76 m depth and major transitions recorded by multiple proxies outside this study have been combined to suggest that core VC-3 was deposited during marine isotope stages (MIS) 14 to MIS 10, including glacial terminations VI (533 ka) and V (424 ka). Alternating field demagnetization response resolves positive inclination magnetizations from samples through most of the core, consistent with Brunhes normal polarity. Three short intervals of shallow to negative inclination magnetizations may partially record geomagnetic polarity events at ~406 ka (11α), ~536 ka (14 α) and the Big Lost excursion (~580 $\pm$ 8 ka). Remanent magnetization in these sediments is principally carried by a range of multidomain to pseudo-single domain ferrimagnetic particles. Sedimentary deposits of glacial period 5 are typified by higher remanent magnetization and susceptibility values and interglacial times are characterized by lower intensity values. Anomalously high magnetic susceptibility and/or rock magnetic intensities measured from 48 m to 43 m are most likely due to the formation of new magnetic phases (i.e., greigite) over a lithologically distinct interval with preserved shallow mud cracks.

INTRODUCTION

A middle Pleistocene lake sequence preserved in the east moat of the Valles caldera, a large volcanic caldera in northern New Mexico, was cored in 2004 (core VC-3; see Fawcett et al., 2007, for discussion of the geologic setting and coring history). Lithology of the VC-3 section is mostly dominated by well-laminated to thinly bedded lacustrine sediment with one sanidine-bearing tephra layer at 76 m. Turbidites up to 1 m thick are present at ~74 m, ~71 m, and ~63 m. Both bioturbation and blocky sedimentary texture are visible from 48 m to 40 m. Large desiccation cracks (up to a meter thick) are indicated at 22 m and 5 m (Fig. 1A). A tentative chronology for core VC-3 is based on an Ar/Ar age determination of 552 ± 3 ka from a tephra near the base of the core (76 m). In addition, major transitions in records of total organic carbon, carbon isotope values, carbon/nitrogen values, pollen, and facies changes at 53 m and 27 m are attributed to glacial terminations VI and V (Fawcett et al., 2007). VC-3 deposition spans three glacial (MIS 14, ~80 m to 53 m; MIS 12, 40 m to 27 m; and MIS 10, 17 m to 5 m) and two interglacial marine isotope stages (MIS 13, 53 m to 40 m; and MIS 11, 27 m to 17 m) (Figs. 1, 2). This contribution focuses on initial rock magnetic and paleomagnetic results from the VC-3 core, based on an average sampling interval of about 20 cm through the entire core, and how these results compare to transitions expressed in proxy records described by Fawcett et al., (2007). Given the age model for deposition of VC-3 sediments, paleomagnetic features in the core can probably be correlated with global field events (11α, 14α, and the Big Lost excursion; Champion et al., 1988; Lund et al., 2001; Singer et al., 2002).

METHODS

Core VC-3 is archived at the LacCore facility at the University of Minnesota – Twin Cities (UMN). U-channel samples taken from 48 core segments (5.52 m to 79.92 m) were transported from UMN to the University of New Mexico (UNM) to facilitate a multiproxy paleoclimate investigation of sediments from the core. U-channel segments were subsequently sampled using nonmagnetic tools and placed into standard paleomagnetic sediment cubes (internal volume of 8 cm^3). Each sediment cube ("sample") was subjected to the following procedures and measurements in the UNM Department of Earth and Planetary Sciences Paleomagnetism Laboratory, listed in order of the measurement: volume susceptibility (κ; measured on a KLY-4S Kappabridge); AF demagnetization of natural remanent magnetization (NRM); acquisition of anhysteretic remanent magnetization (ARM) in a peak AF field of 95 mT and a DC field of 0.1 mT; AF demagnetization of ARM; sequential acquisition and back-field DC demagnetization of saturation isothermal remanence magnetization (SIRM); and AF demagnetization of SIRM.

The rock magnetic experiments following AF demagnetization of NRM provide information on the types of magnetic phases, relative concentrations, and coercivity distributions of the magnetic particles capable of carrying a remanence in the sediments (Thompson and Oldfield, 1986; Verosub and Roberts, 1995; Evans and Heller, 2003). ARM and SIRM are both types of laboratory-induced, permanent magnetizations produced by exposing a sample to an external magnetic field. In the case of ARM a sample is placed in a demagnetizing field (95 mT) that decays to zero while a biasing DC field (100 mT) is applied to activate magnetic components whose coercivities are equal to or less than 100 mT (e.g., magnetite). SIRM acquisition in successively increasing direct fields (as high as 3 T) is high enough to saturate all ferrimagnetic material and measure the range in coercivity (or hardness) in VC-3 samples. Hysteresis parameters were measured with a room-temperature vibrating sample magnetometer at the Institute for Rock Magnetism at UMN.

In addition, magnetic separates were obtained from sediment fractions taken at 65 m, 30.5 m, 18.1 m, and 10.3 m, by disaggregating the sediment in isopropyl alcohol and passing a Sm-Co alloy magnet over the slurry. The magnetic extracts were imaged using a JEOL 5800LV scanning electron microscope (SEM) equipped with an Oxford Analytical ultra thin-window energy dispersive spectroscopy (EDS) and an Oxford Isis 300 X-ray analyzer for visual and chemical identification of magnetic particles. EDS data provide a first-order estimate of relative elemental concentrations for a given grain but cannot be used to distinguish between the oxidation states of iron.

RESULTS

Paleomagnetism

Results of this study are discussed in the context of an inferred age model proposed by Fawcett et al. (2007), where VC-3 deposition spans the three glacial and two interglacial marine isotope stages noted above (Figs. 1, 2). The paleomagnetic and rock magnetic data should be considered preliminary, as many critical intervals of the VC-3 core have not been analyzed with sufficient spatial resolution.

NRM intensities from sediments deposited during glacial times range from 0.04 mA/m to 1.6 mA/m, whereas lower intensity values 0.05 mA/m to 0.2 mA/m are typical of interglacial times (Fig. 1C). Maximum NRM intensity values, as high as 3.3 mA/m, are found over a depth interval (43 m to 48 m) previously described by Fawcett et al. (2007) as a distinct lithologic facies containing shallow mudcracks (Fig. 1A).

The behavior of AF demagnetization response of NRM ranges from well-defined single- and multi-component vector paths that decay to the origin (Fig. 3C), to poorly defined vector paths that do not decay to the origin (Fig. 3E). Principal component analysis (PCA, Kirshvink, 1980) reveals a wide range of maximum angular deviation (MAD) values. The demagnetization data were grouped into three categories (using unanchored line segments with at least five data points) based on quality of response (Fig. 3B): good (MAD < 10), moderate (10 < MAD < 20), and poor (MAD > 30). Magnetizations isolated in progressive demagnetization are typically of positive inclination, regardless of overall response. We have identified two intervals of negative inclination recorded in samples of high to moderate demagnetization data quality at 17 m (Fig. 4A) and 67 m (Fig. 4B). One additional interval of negative inclination defined by adjacent samples of poor demagnetization quality is at about 79 m (Fig. 4C).

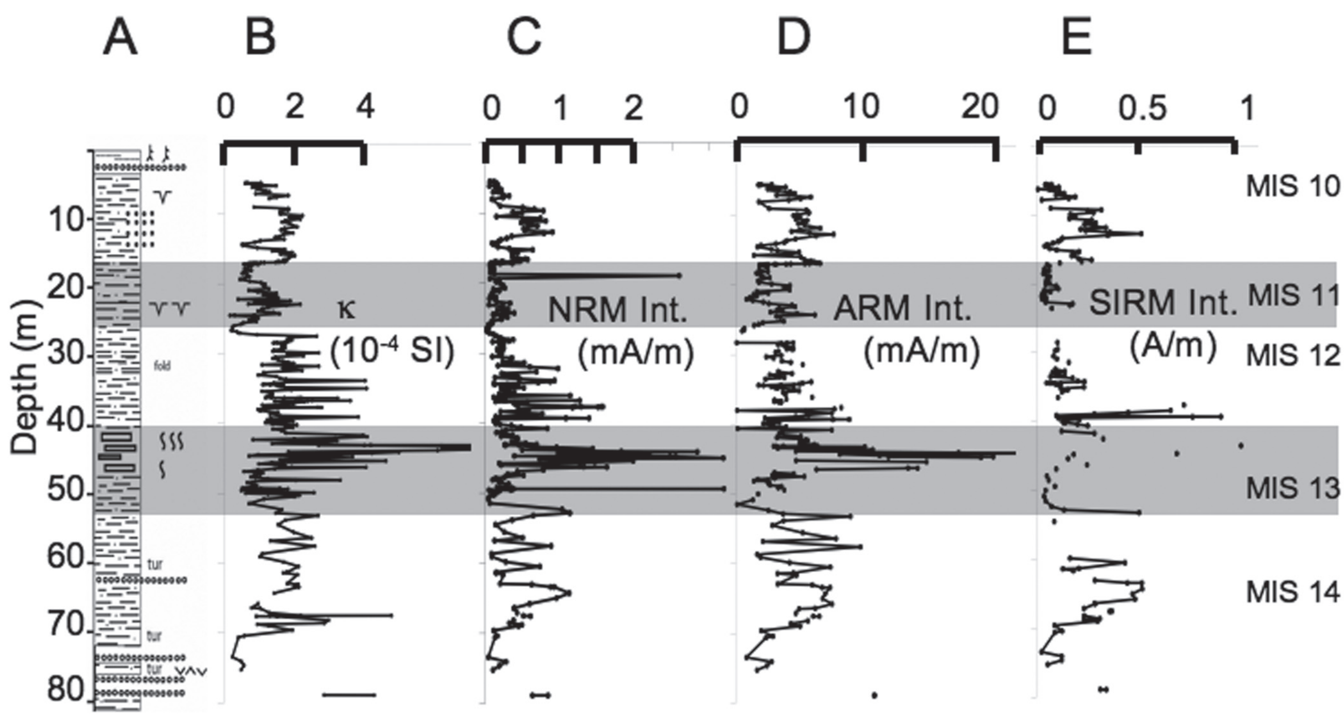

FIGURE 1. Compliation of the VC-3 core, summarizing some common rock magnetic properties. A. Lithology of VC-3 sediments mostly well laminated to thinly bedded lacustrine sediment and one tephra layer at 76 m. Depth intervals composed of turbidites are indicated with "tur" labels next to the sediment column. Sandy intervals are illustrated by small circles in a horizontal line between 80 m and 60 m. Bioturbation and blocky sedimentary texture is illustrated from 48 m to 40 m. A fold is preserved at ~ 32 m. Large desiccation cracks are indicated at 22 m and 5 m. B. Volume susceptibility, reflecting concentration of magnetic minerals. C. Intensity of natural remanent magnetization reflecting the degree to which particles align with the Earth's magnetic field. D. Intensity of anhysteretic remanent magnetization achieved by activating the soft (e.g., magnetitie) coercivity fraction of magnetic phases present in VC-3 sediments. E. Intensity of saturation isothermal remanence magnetization acquired from a laboratory induced magnetization (applied field of 3 T) that activates ferrimagnetic mineral phases. Each record shows larger magnetic remanence intensity values during glacial intervals than interglacial intervals with the exception of very high values over a lithologically distinct interval of sedimentation 48 m to 43 m.

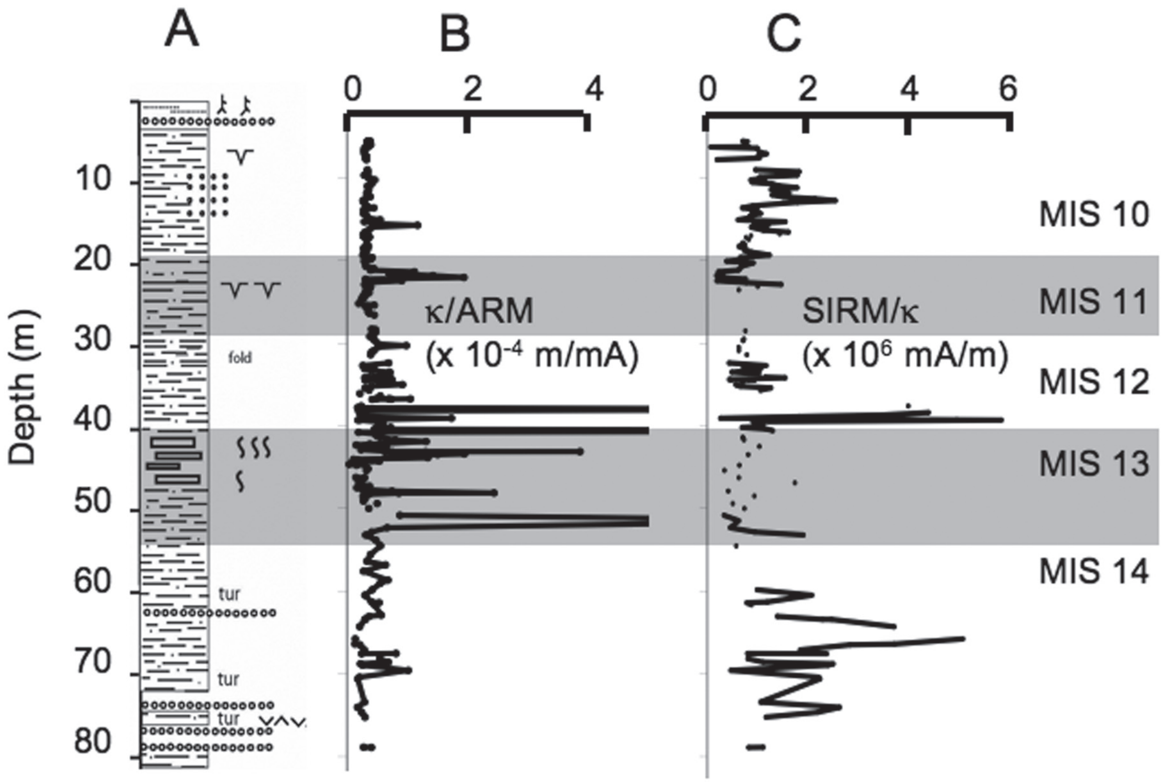

FIGURE 2. A. Lithology of VC-3 sediments (See Fig. 1 caption for deteails). B. Plot of volume susceptibility normalized anhysteretic remanence magnetization reflecting changes in mineralogy. C. Saturation isothermal remanent magnetization normalized by mass susceptibility provides a first order identification of intervals that may contain greigite. Changes in magnetic mineralogy illustrated by these plots is not consistent with marine isotope stage boundaries.

Rock magnetism

Environmental magnetic studies frequently use patterns of remanence intensity with depth to identify the dominant magnetic phases that contribute to the NRM (Verosub and Roberts, 1995; Evans and Heller, 2003). Intermediate volume susceptibility (κ) values were recorded during glacial intervals MIS 10 (~1.8 x 10^{-4} SI), MIS 12 (~2.5 x 10^{-4} SI), and MIS 14 (~1.7 x 10^{-4} SI) (Fig. 1B). Results of κ from interglacial stages are typically 1.1 x 10^{-4} SI for both MIS 11 and MIS 13. The maximum observed κ value 1.3 x 10^{-3} SI was identified during MIS 13 at about 43 m depth where shallow mudcracks and blocks of reddish sediment are present (Figs. 1A, B).

High ARM intensity values were recorded from sediment deposited over glacial intervals (0.8 mA/m to 9.5 mA/m), lower intensity values (0.8 mA/m to 4.1mA/m) representative of interglacial depositional environments, and anomalous intensity values (0.8 mA/m to 29 mA/m) over a lithologically distinct interval between 48 m and 43 m (Fig. 1D). SIRM intensity values again record higher intensity values in sediments deposited during glacial intervals (0.02 mA/m to 0.9 mA/m) than sediments deposited during interglacial times and the highest intensity values (1.04 mA/m) recorded between 48 m to 43 m (Fig. 1E).

Normalized magnetization parameters, such as κ /ARM intensity, are used in an attempt to identify changes in magnetic mineralogy through a sediment column (Fig. 2B). Most κ /ARM values vary between 2 x 10^{-5} m/mA and 5 x 10^{-5} m/mA for most of the core with the following exceptions. At around 52 m and between 48 m to 43 m (the lithologically distinct interval previously mentioned) the values of κ/ARM vary by an order of magnitude from 1.3 x 10^{-4} m/mA to 1.4 x 10^{-3} m/mA. High κ/ARM values of 1.2 x 10^{-4} m/mA and 1.9 x 10^{-4} m/mA are recorded over depth intervals (~5 m to ~6 m and 21 m to 22 m, respectively) associated with preserved mudcracks (Fig. 2B). High values of SIRM intensities normalized by κ provide an indicator for griegite (Roberts, 1995). Most SIRM/κ values collected to date (Figure 2C) vary between 4.6 x 10^5 mA/m and 8.2 x 10^5 mA/m, but high SIRM/κ values were observed over several depth intervals, including 5.1 x 10^6 at ~65 m, 5.9 x 10^6 mA/m at about 40 m, and 2.4 x 10^6 mA/m at ~ 13 m. Depth intervals that yield high SIRM/χ ratios, which may indicate the presence of greigite, do not coincide with transitions associated with interpreted MIS boundaries.

IRM acquisition curves for samples from a wide range of depths typically show full saturation by 1 T, and at least a 10% IRM increase beyond 0.3 T. Backfield demagnetization of IRM yields coercivity of remanence (H_{cr}) values typical of magnetite (< 0.1 T, Fig. 5).

The shape of a hysteresis loop (Fig. 6), measured while sequentially exposing a sample to both positive and negative saturating fields, is defined by saturation remanence (ability of a sample to

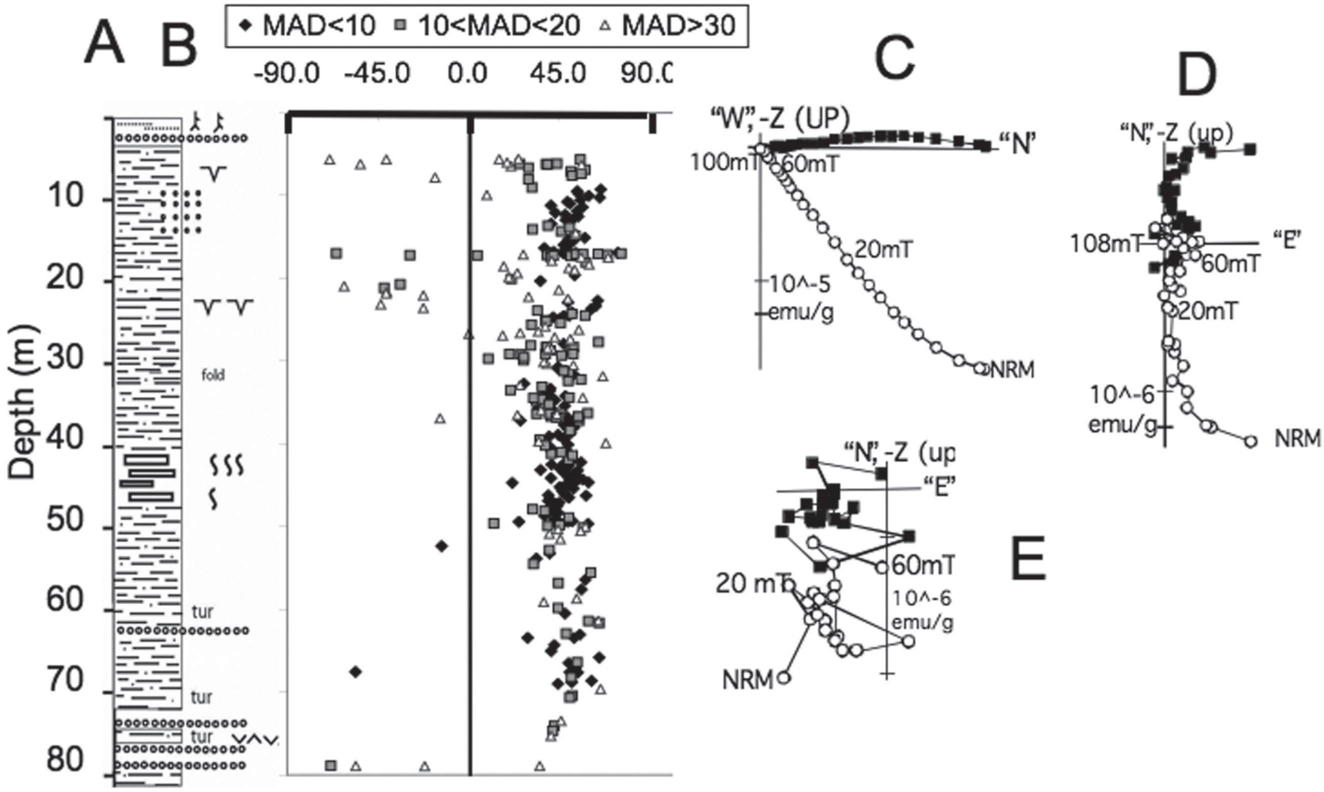

FIGURE 3. A. Lithology of VC-3 sediments (See Fig. 1 caption for details). B. Magnetization inclination results, with diamonds representing high quality data (maximum angular deviation (MAD) values less than 10°), squares representing moderate quality data (MAD values between 10° and 20°), and triangles representing poor quality data (MAD values greater than 20°). Three intervals with negative inclination magnetizations isolated (with at least 5 points between 20 and 65 mT) are shown at 16.92 m to 17.24 m, 67.54 m to 67.56 m, and 78.88 m to 78.89 m. C-E. Examples of orthogonal vector demagnetization diagrams (Zijderveld, 1967) of good (C), moderate (D), and poor demagnetization response (E).

hold a magnetization) and coercivity (the hardness or stability of a remanence against reverse-polarity applied fields) of the magnetic phases present in a sample. A hysteresis loop with a constricted or wasp-waisted shape (e.g., Fig. 6A) indicates a mixture of magnetic phases. Figure 6B shows hysteresis behavior typical of fine-grained magnetite (Evans and Heller, 2003). Three principal parameters measured by hysteresis loops include saturation of remanence (M_{rs}), magnetization in the presence of a saturating field (M_s), and the field strength required to reduce magnetization to zero (H_c). These parameters are commonly interpreted in terms of ratios: M_{rs} is normalized by M_s (remanence ratio) and H_{cr}, obtained from backfield demagnetization of IRM, is normalized by H_c (coercivity ratio). A Day plot of coercivity versus remanence ratios is used to estimate grain sizes present in a magnetic population (Day et al. 1977). Data from remanence and coercivity ratios of VC-3 sediments indicate a grain size distribution of pseudo-single domain and multidomain grains. Because remanence and coercivity values do not follow a single path, VC-3 sediments most likely contain a mixture of more than one dominant magnetic phase (Fig. 7).

SEM observation and EDS analysis on magnetic separates shows the common magnetic phase in these extracts is a titanium-bearing iron oxide (i.e., titanomagnetite, Figs. 8A, D). The separates include titanium-bearing iron oxide grains coated with silica and crusted with magnetite overgrowths (Fig. 8A), titanium-bearing iron oxide grains with clear evidence of high temperature oxidation/exsolution lamellae (most commonly ilmenite; Fig. 8B), maghemite with surface cracks, hematite, and iron sulfides (presumably greigite because of the botryoidal habit observed from the SEM images) (Fig. 8D).

DISCUSSION

All paleomagnetic and rock magnetic data are discussed in the context of the age model described by Fawcett et al. (2007), based on characterization of lithologic facies changes, percent total organic carbon, carbon isotopic variation, and trends in carbon/nitrogen values through the core. Major transitions in these proxies at 53 m and 27 m and an Ar/Ar age determination of 552 ± 3 ka were combined to interpret VC-3 sedimentation as spanning three glacial marine isotope stages (MIS 10, 12, and 14) and two interglacial MIS stages (MIS 11 and 13).

Interpretations of paleomagnetic and rock magnetic records of lacustrine sediments are subject to numerous uncertainties

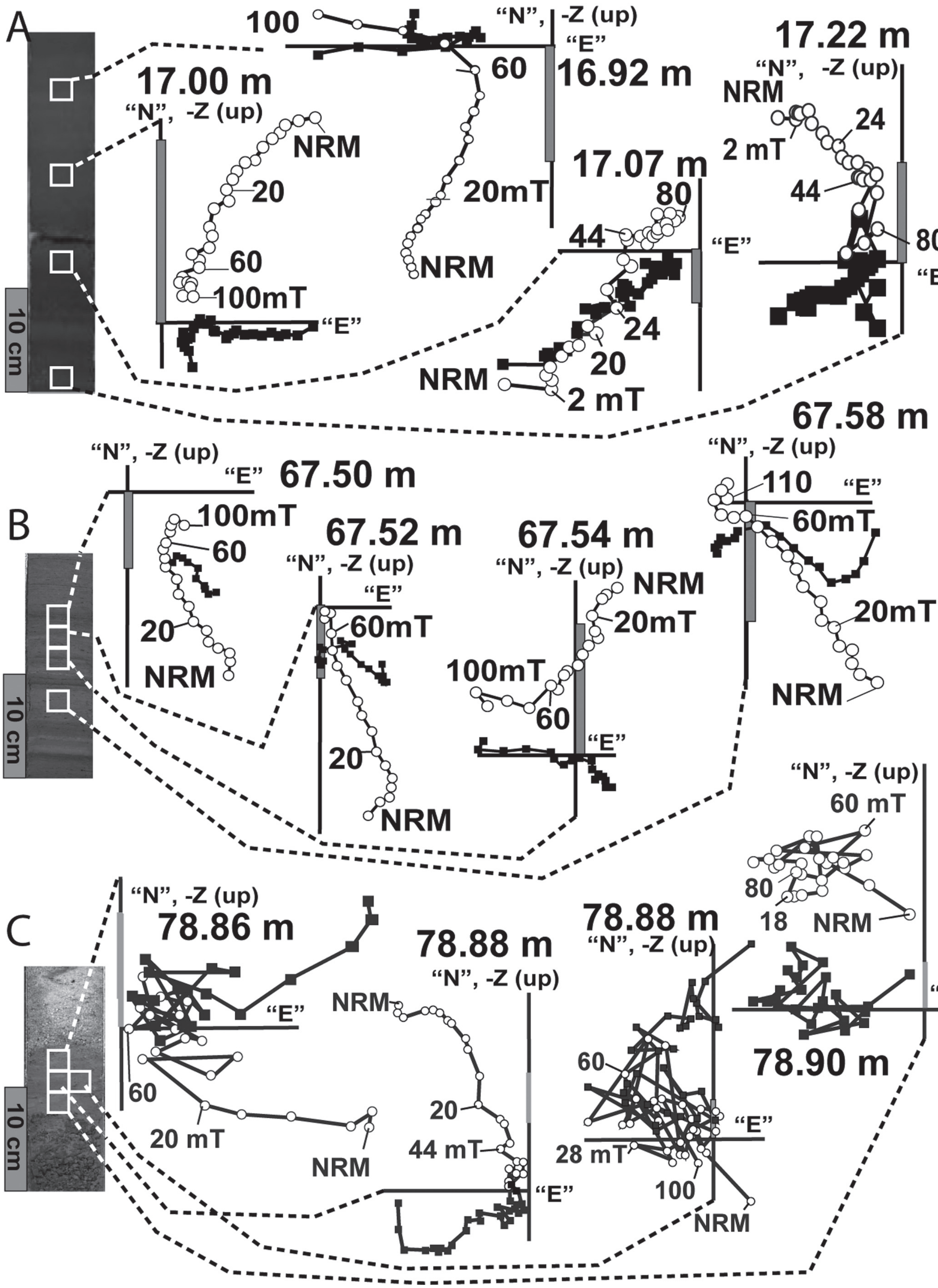

FIGURE 4. Picture of parts of VC-3 core segments with sampling location and orthogonal vector demagnetization diagrams of those samples with open (closed) symbols represent projections onto the vertical (artificial horizontal) planes. Peak demagnetization fields are shown for selected vertical projection data. A. Progressive step-wise alternating field demagnetization of natural remanence magnetization (NRM) from samples taken from 16.92 m to 17.24 m depth. B. Negative magnetization inclination results from progressive alternating field demagnetization from sediments at 67.54 m to 67.56 m depth. C. Poorly defined negative magnetization results from samples at 78.88 m to 78.89 m depth. Laminated sediment samples for this study are overlain by a lithologicaly distinct sandy interval.

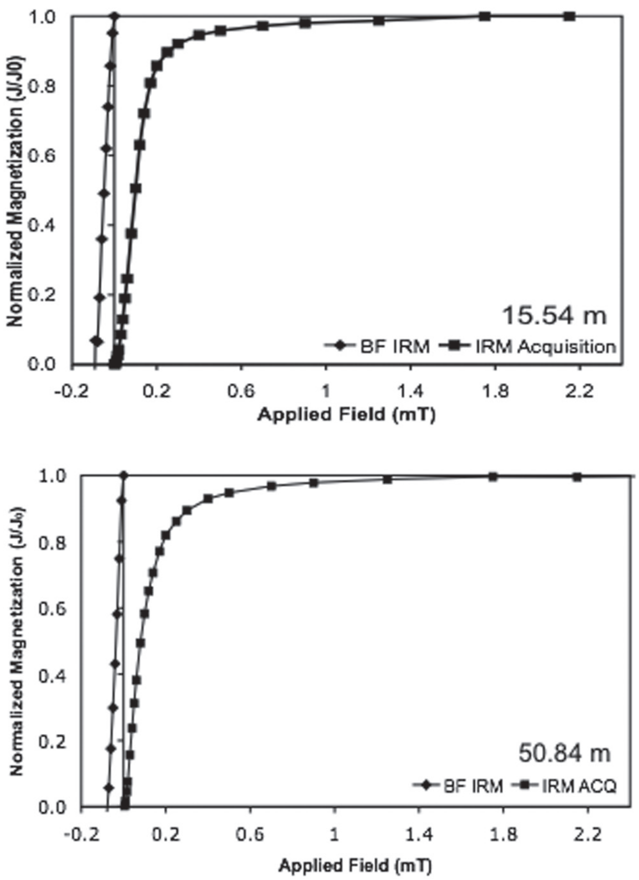

FIGURE 5. Isothermal remanent magnetization (IRM) curves showing saturation at or near ~1.6 T and backfield demagnetization of IRM shows coercivity of remanence (H_{cr}) values less than 0.1 T, which demonstrates an influence by a high coercivity phase.

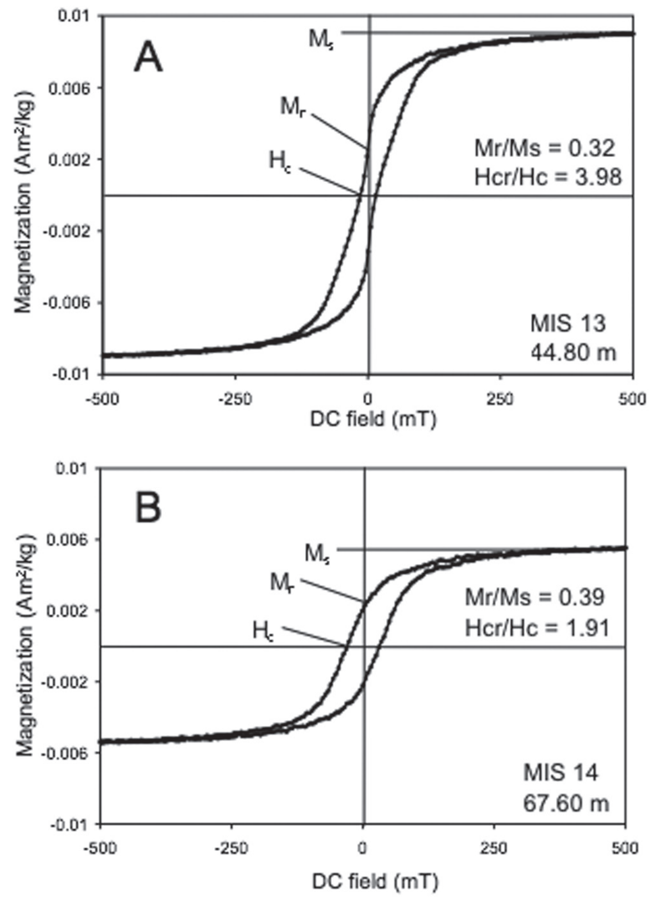

FIGURE 6. Hysteresis loops result from sequential exposure of a sample to both positive and negative saturating fields. A. Constricted loop from a sample at 44.8 m (interglacial MIS 13) indicating a mixture of magnetic phases. B. Hystersis loop from a sample at 67.7 m depth (glacial MIS 14) typical for sample with magnetite as the dominant remanence carrier.

concerning diagenetic processes that may modify original detrital minerals and/or precipitate new magnetic phases (Collinson, 1965; Irving and Major, 1964; Stacy, 1972; Verosub, 1977; Butler, 1992). Nonetheless, theoretical studies and laboratory experiments have demonstrated that sediments do have the potential to be high fidelity recorders of the geomagnetic field. For most of the VC-3 core, sample inclinations resolved during progressive AF demagnetization are consistent with positive inclination magnetizations expected from magnetic particle-bearing sediment deposited during the Brunhes chron (Champion et al., 1988; Langereis et al., 1997; Singer et al., 2002). However, three intervals of negative inclination magnetizations are recorded at 16.92 m to 17.24 m, 67.54 m to 67.56 m, and 78.88 m to 78.92 m (Fig. 9).

The most robust and longest recorded inferred geomagnetic polarity event (Fig. 4A) within VC-3 core sediments is characterized by negative inclination magnetizations from 16.92 m to 17.24 m and lies about 10 m above glacial termination V (424 ka; Lisiecki and Raymo, 2005; Fawcett et al., 2007), consistent with excursion 11α (~406 ka) recorded in sediments from ODP leg 172 (Lund et al., 2001). The second inferred geomagnetic field event is only recorded in one sample from 67.54 m to 67.56 m (Fig. 4B) and lies 16 m below glacial termination VI (533 ka; Lisiecki and Raymo, 2005; Fawcett et al., 2007). The first documented reversal prior to 533 ka is 14α (~536 ka; Lund et al., 2001). The Calabrian Ridge II polarity event (Langereis et

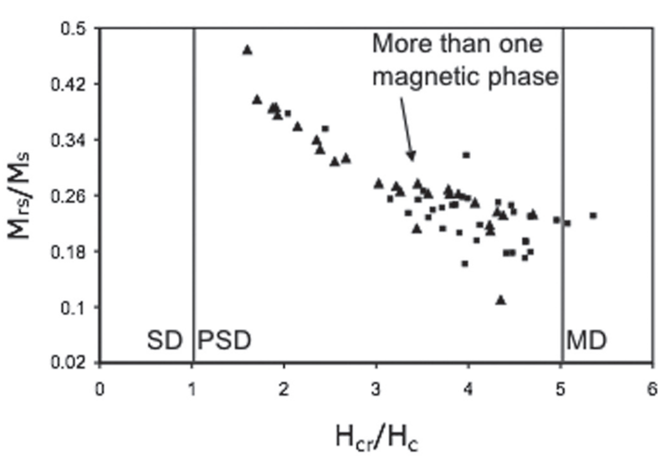

FIGURE 7. Plot of coercivity versus remanence ratios (Day et al., 1977) suggesting no clear difference in grain size or mineralogy of sediments deposited during glacial (triangles) and interglacial (squares) times. VC-3 sediments do not plot along a single curve, indicating a contribution by more than one magnetic phase.

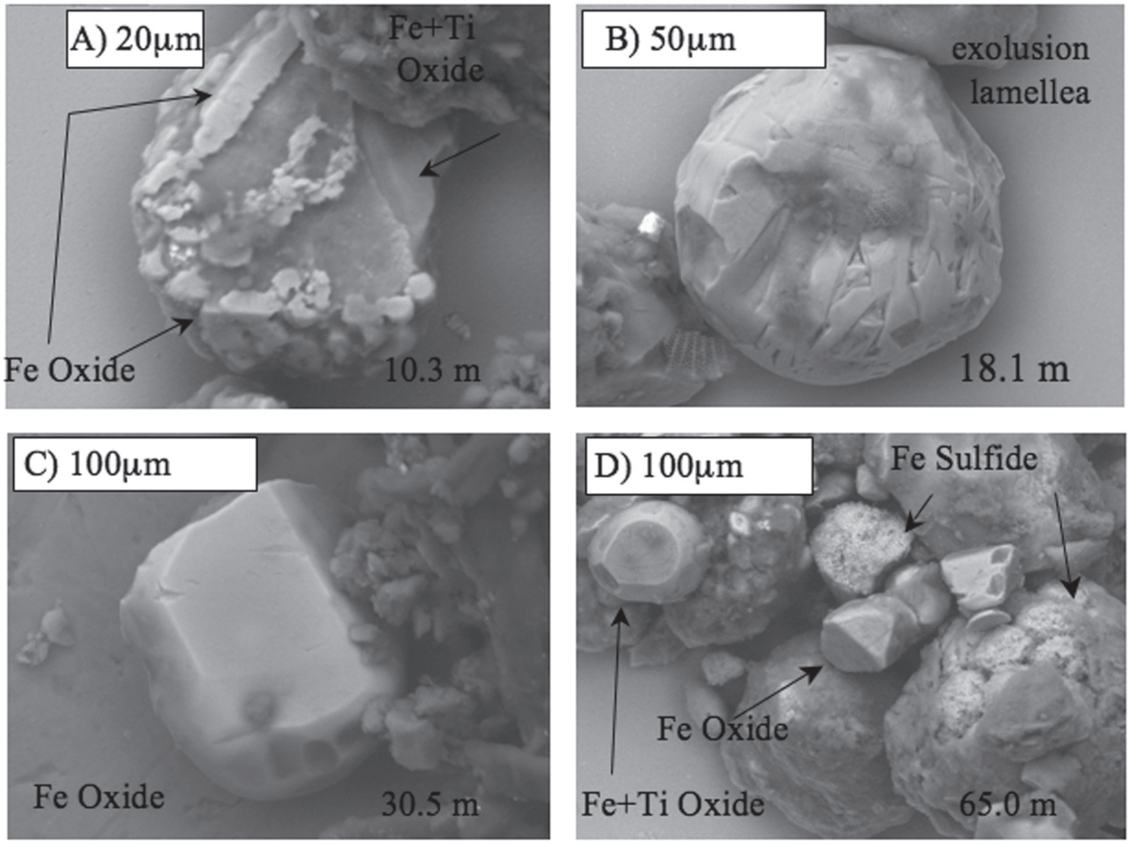

FIGURE 8. SEM photomicrographs of magnetic separates showing magnetic grain types present in VC-3 sediments. A. Titanium-bearing iron oxides with a silica rich coating and iron oxide. B. Titanium-bearing grain displaying exsolution lamellae (commonly composed of illmenite) indicative typical volcanic rock source. C. Subhedral iron oxide grain. D. Oxide grains include euhedral iron oxide, rounded titanium-bearing oxide, and botryoidal iron sulfides.

al., 1997) occurs at ~513 ka and should be expressed in VC-3 sediments at about 4 m, using the average sedimentation rate of ~0.25 mm/yr (Fawcett et al., 2007). Anomalous magnetic phases between 43 m and 48 m observed in the environmental magnetic records of VC-3 sediments indicate the natural remanent magnetization may have been overprinted by the formation of authigenic greigite. The Calabrian Ridge II event (Langereis et al., 1997) is not recorded in VC-3 core sediments owing to distinct magnetic phases identified through numerous rock magnetic records from 48 m to 43 m. The third potential geomagnetic field event recorded in VC-3 sediments is poorly isolated by progressive AF demagnetization of NRM. However, three adjacent samples, about 3.2 m below the sanidine-bearing tephra horizon that yields an Ar/Ar age of 552 $\pm$ 3 ka (Fawcett et al., 2007), display negative inclination vector paths (Fig. 4C). High sedimentation rates in the deepest part of the core, owing to rapid initial infilling of the caldera catchment, suggest the polarity event at ~79 m is too young to correlate to the Big Lost polarity feature (Champion et al., 1988; Singer et al., 2002). The Big Lost polarity feature has been recorded in both sediments recovered from ODP Leg 172, Blake and Bahamas Outer Ridge, western North Atlantic, (15α, Lund et al., 2001), basalt flows at La Palma, Canary Islands, (~ 565 $\pm$ 28 ka; Champion et al., 1988), and basalt flows in the Snake River Plain, Idaho, (~580 $\pm$ 8 ka; Singer et al., 2002). It is, however, likely that the interval recording negative inclination magnetization is from a stratigraphically isolated interval of fine-grained mud disconformably overlain by a sandy interval below the sanidine-bearing tuffaceous sediment (Fig. 4C), in which case the lowermost interval of negative inclinations does correlate to the Big Lost event.

Patterns of variations in environmental magnetic data, including concentration dependent and grain-size/mineralogy-dependent rock magnetic parameters, indicate higher (relative) concentrations of magnetic phases deposited during glacial times, whereas lower concentrations of magnetic phases are reported from times of interglacial sediment deposition. This observation supports the conclusions of Fawcett et al. (2007), that glacial periods are associated with wetter climates and lower lake productivity, while interglacial periods are typified by drier climates, higher lake productivity (Figs. 1, 2). A limited range of source rocks (mostly rhyolites of the Valles Caldera resurgent domes and moat eruptions) provide most of the terrigenous sediment supply of Valle Grande lake deposits. Additionally, organic carbon and biogenic silica are also identified in core VC-3 (Fawcett et al., 2007). Multiple lines of evidence (rock magnetic data, including hysteresis and biparametric plots, and inspection of magnetic separates) suggest sediments have undergone alteration and include the following magnetic phases: homogeneous titanomag-

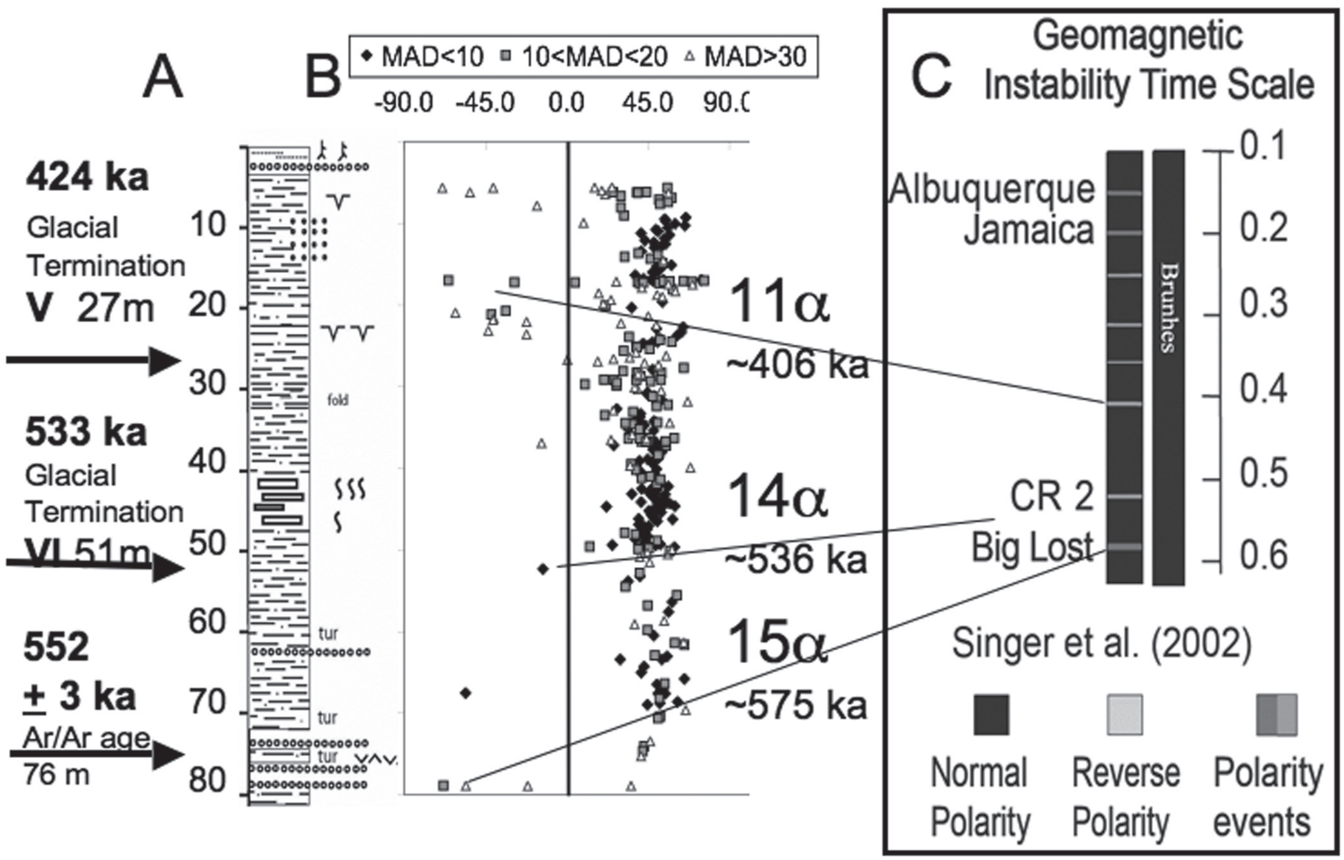

FIGURE 9. A. Lithology of VC-3 sediments (see caption of Fig. 1 for sediment description), shown with interpreted glacial terminations V and VI, and Ar/Ar age determination from Fawcett et al., (2007). B. Paleomagnetic inclination values, isolated by alternating field demagnetization, grouped by data quality (see Fig. 3). C. Correlation of negative inclination intervals to geomagnetic field events described in Lund et al., (2001) and Singer et al., (2002).

netite, nearly pure magnetite, maghemite, and titanomagnetite with exsolution lamellae most commonly associated with ilmenite. The Valle Grande lacustrine system experienced reducing conditions, in the presence of sulfur, that led to authigenic growth of magnetic sulfide phases, which are most notable from 43 m to 48 m, but also present to some degree at ~65 m, between 48 m and 40 m, 21 m to 22 m, ~ 13 m, and ~5 m.

SUMMARY

Preliminary paleomagnetic and rock magnetic records from the VC-3 core, typically defined at a spatial resolution of about 20 cm, reveal three intervals of negative inclination magnetizations at 16.92 m, 67.54 m, and 78.88 m recorded in a mixture of titanomagnetite, with and without ilmenite exsolution lamellae, magnetite, and minor hematite. Given the highly variable sedimentation rates associated with VC-3 deposition, each interval of negative inclination is consistent with published geomagnetic polarity events, 11α, 14α, and the Big Lost, supporting the proposed age model of Fawcett et al. (2007) for VC-3 sedimentation. Overall trends in environmental magnetic properties reveal higher intensity values (NRM, 0.05 mAm to 0.2 mAm; ARM, 0.8 mAm to 4 mAm; SIRM, 0.03 Am to 1.4 Am; κ, 2.1 x 10^{-4} SI) during wetter times (glacial MIS 14, 12, and 10) and deeper lake conditions, whereas lower intensity values (NRM, 0.04 mAm to 1.6 mAm; ARM, 0.8 mAm to 8 mAm; SIRM, 0.02 Am to 0.9 Am; κ, 1.1 x 10^{-4} SI) recorded during drier times are consistent with deposition during interglacial (MIS 13 and 11) times. Rock magnetic results indicate a distinct assemblage of magnetic phases most notably recorded in sediments deposited from 43 m to 48 m, including an unidentified magnetic sulfide phase, most likely greigite. Additional magnetic experiments and comparison of rock magnetic data with bulk geochemistry and XRD data are needed to further identify magnetic mineral phases present in VC-3 sediments and test the degree to which magnetic phase changes are related to climatic variations.

ACKNOWLEDGMENTS

We thank the Institute of Geophysics and Planetary Physics (IGPP) at Los Alamos National Laboratory, which provided funding for most of the work described in this study. The Institute for Rock Magnetism at the University of Minnesota – Twin Cities provided a partial visiting fellowship for travel to Minnesota and use of their equipment. This work has also been partially funded through graduate student scholarships from the Department of Earth and Planetary Sciences, University of New Mexico. We are grateful to Mike Jackson, Institute for Rock Magnetism, and Joe Rosenbaum, U.S.Geological Survey, Denver, for their insightful comments for improvement of this manuscript.

REFERENCES

Butler, R. F., 1992, Paleomagnetism: magnetic domains to geologic terranes: Boston, Blackwell Scientific Publications, 238 p.

Champion, D. E., Lanphere M. A., and Kuntz, M. A., 1988, Evidence for a new geomagnetic reversal from lava flows in Idaho: discussion of short polarity reversals in the Brunhes and Late Matuyama polarity chrons: Journal of Geophysical Research, v. 93, p. 11,667-11,680.

Collison, D. W., 1965, Depositional remanent magnetization in sediments: Journal of Geophysical Research, v. 70, p. 4663-4668.

Day, R., Fuller, M., and Schmidt, V. A., 1977, Hysteresis properties of titanomagnetites; grain-size and compositional dependence. Chemical and physical problems in paleomagnetic field determinations: International Association of Geomagnetism and Aeronomy interdisciplinary symposium SM-3, Grenoble, France, p. 260-267.

Evans, M. E., and Heller, F., 2003, Environmental magnetism. Amsterdam, Academic Press, 293p.

Fawcett, P. J., Heikoop, J., Goff, F., Anderson, R. S., Donohoo-Hurley, L., Geissman, J. W., WoldeGabriel, G., Allen, C. D., Johnson, C., Smith, S.J., and Fessenden-Rahn, J., 2007, Two middle Pleistocene glacial-interglacial cycles from the Valle Grande, Jemez Mountains, northern New Mexico: New Mexico Geological Society, 58th Field Conference, Guidebook, p. 409-417.

Irving, E., and Major, A., 1964, Post-depositional detrital remanent magnetization in a synthetic sediment: Sedimentology, v. 3, p. 135-143.

Johnson, H. P., Lowrie, W., and Kent, D.V., 1975, Stability of anhysteretic remanent magnetization in fine and coarse magnetite and maghemite particles: The Geophysical Journal of the Royal Astronomical Society, v. 41, p. 1-10.

King, J., Banerjee, S., Marvin, J., and Ozdemir, O., 1982, A comparison of different magnetic methods for determining the relative grain size of magneitite in natural materials: some results from lake sediments: Earth and Planetary Science Letters, v. 59, p. 404-419.

Kirschvink, J. L., 1980, The least-squares line and plane and the analysis of paleomagnetic data: examples from Siberia and Morocco: Geophysical Journal of the Royal Astronomical Society, v. 62, p. 699-718.

Langereis, C. G., Dekkers, M. J., de Lange, G. J., Paterne, M., and Santvoort, P. J. M., 1997, Magnetostratigraphy and astronomical calibration of the last 1.1 Myr from an eastern Mediterranean piston core and dating of short events in the Brunhes: Geophysical Journal International, v. 129, p.75-94.

Lisiecki, L. E., and Raymo, M. E., 2005, A Pliocene-Pleistocene stack of 57 globally disturbed benthic delta (super 18) O records: Paleoceanography, v. 20, doi:10.1029/2004PA00107.

Lund, S. P., Williams, T., Acton, G. D., Clement, B., and Okada, M., 2001, Brunhes chron magnetic field excursions recovered from Leg 172 sediments: Proceedings of the Ocean Drilling Project, Scientific Results, v. 172, p. 1-18.

Roberts, A. P., 1995, Magnetic properties of sedimentary greigite (Fe_3S_4): Earth and Planetary Science Letters, v. 134, p. 227-236.

Singer, B. S., Relle, M. K., Hoffman, K. A., Battle, A., Laj, C., Guillou, H., and Carracedo, J. C., 2002, Ar/Ar ages from transitionally magnetized lavas on La Palma, Canary Islands, and the geomagnetic instability timescale: Journal of Geophysical Research v. 107, n. B11, p. 1-20.

Stacy, F. D., 1972, On the role of Brownian motion in the control of detrital remanent magnetization in sediments: Pure Applied Geophysics, v. 98, p. 139-145.

Tarling, D. H., and Hrouda F., 1993, The magnetic anisotropy of rocks: London, Chapman and Hall, 217 p.

Thompson, R., and Oldfield, F., 1986, Environmental magnetism: Boston, Allen & Unwin, 227 p.

Verosub, K. L., 1977, Depositional and post-depositional processes in the magnetization of sediments: Review of Geophysical Space Physics, v. 15, p. 129-143.

Verosub, K. L., and Roberts A. P., 1995, Environmental magnetism: past, present, and future: Journal of Geophysical Research, v. 100, no. B2, p. 2175-2192

Zijerveld, J.D.A., 1967, A. C. demagnetization of rocks, *in* Collinson, D. W., Creer, S. K., and Runcorn, K., eds., Methods in paleomagnetism: Amsterdam, Elsevier, p. 254-286.